Absence of Photoinduced Charge Transfer in Blends of PbSe Quantum Dots and Conjugated Polymers

Kevin M. Noone, Nicholas C. Anderson, Noah E. Horwitz, Andrea M. Munro, Abhishek P. Kulkarni, and David S. Ginger*

Department of Chemistry, University of Washington, Box 351700, Seattle, Washington 98195-1700

ABSTRACT We use photoluminescence (PL) quenching and photoinduced absorption (PIA) spectroscopy to study charge transfer in bulk heterojunction blends of PbSe quantum dots with the semiconducting polymers poly-3-hexylthiophene (P3HT) and poly[2-methoxy-5-(3′,7′-dimethyloctyloxy)-*para*-phenylene vinylene] (MDMO-PPV). PIA spectra from the PbSe blends are compared to spectra from similar blends of the polymers with phenyl-C_{61}-butyric acid methyl ester (PCBM) and blends with CdSe quantum dots. We find that the MDMO-PPV PL is quenched, and the PL lifetime is shortened upon addition of PbSe quantum dots, while the PL of the P3HT is unaffected upon blending. However, for PbSe blends with both polymers, the PIA spectra show very little polaronic signal, suggesting that few, if any, long-lived charges are being produced by photoinduced charge transfer.

KEYWORDS: lead selenide · nanocrystal · charge transfer · bulk heterojunction · Förster energy transfer · organic solar cell · photovoltaics

Organic semiconductors that can be processed from solution into flexible thin films have emerged as attractive materials for use in low-cost solar cells.[1] Colloidal semiconductor nanocrystal quantum dots can also be processed from solution and incorporated into devices ranging from light-emitting diodes[2−4] to solar cells[5−15] while retaining some of the traditional advantages of bulk inorganic materials such as increased photostability, broad absorption spectra, and mobilities approaching 1 $cm^2/(V \cdot s)$.[9,16] Additionally, the band gaps of quantum dots are size-tunable, permitting chemical control over the energies of their conduction and valence bands, much as the energy levels of organic materials can be tailored *via* chemical substitution. Though there are few presently available organic semiconductors with band gaps that can be tuned to harvest the large fraction of solar radiation falling in the infrared, colloidal quantum dots with band gaps spanning 1000−2000 nm are easily synthesized,[17−19] making them attractive materials for solution processable infrared sensitizers in optoelectronic devices.[11−15] More recently, colloidal quantum dots have attracted increased interest due to reports of multiple exciton generation from absorption of a single photon,[20,21] though the efficiency of this process is a matter of current debate.[22−26]

Currently, the most efficient reported organic solar cells are bulk heterojunction cells based on polymer blends, with power conversion efficiencies greater than 5%.[27] Similar structures using colloidal quantum dots as electron acceptors and sensitizers have shown promise, and blending conjugated polymers such as alkoxy-PPVs and polythiophenes with semiconductor quantum dots is an easy and attractive way to incorporate them into functional photodiodes. Already, bulk heterojunction blends of CdSe quantum dots,[5] nanorods,[6] tetrapods,[7] and starbursts[8] with regioregular poly-3-hexylthiophene (P3HT) have achieved power conversion efficiencies as high as 2% and external quantum efficiencies (EQEs) of 55%.[6] However, efficient photodiodes utilizing blends of conjugated polymers with IR-absorbing quantum dots, such as PbSe, have proven more elusive. Bulk heterojunction devices incorporating blends of PbSe quantum dots and conjugated polymers have produced only 0.1% reported overall power conversion efficiency with less than 5% EQE in the visible and much lower EQE in the infrared.[11,12] While researchers have had success with IR band gap quantum dots in structures such as Schottky diode cells[28−33] and tandem cells,[34] it is still not clear why bulk heterojunction blend devices based on CdSe and PbSe quantum dots exhibit such widely differing efficiencies.

A successful bulk heterojunction solar cell consists of a blend of two materials that form a type-II heterojunction so that photoinduced charge separation takes place at the interface between the

*Address correspondence to ginger@chem.washington.edu.

Received for review December 18, 2008 and accepted April 27, 2009.

Published online May 18, 2009.
10.1021/nn800871j CCC: $40.75

materials.[35] The resulting blend must have sufficient internal surface area so that a majority of photoexcitations can encounter a donor/acceptor interface, and the photoinduced charges generated at the interfaces must also be sufficiently long-lived so that they can be collected before they recombine. It is not clear if blends of PbSe quantum dots with commonly studied polymers meet these criteria. For instance, it is difficult to determine if PbSe forms a type-II heterojunction with the commonly studied polymers P3HT and poly[2-methoxy-5-(3′,7′-dimethyloctyloxy)-*p*-phenylene vinylene] (MDMO-PPV) by simply consulting reported redox potentials. Not only are the reported values for the conduction band of colloidal PbSe quantum dots scattered from 5.2 to 4.2 eV[11,12,36,37] relative to vacuum but also, due to interfacial chemistry and interactions between the materials in blends, the relative alignment of two materials when blended in working solid-state devices can differ from those estimated from cyclic voltammetry in solution or photoelectron spectroscopy measurements on thin films of the pure materials.[38,39]

In this paper, we use photoluminescence (PL) and photoinduced absorption (PIA) spectroscopies to determine if long-lived photoinduced charge transfer occurs between PbSe quantum dots and the widely studied polymers P3HT and MDMO-PPV. We compare these polymer/PbSe blend spectra to PIA spectra obtained from blends of each polymer with phenyl-C_{61}-butyric acid methyl ester (PCBM) and also to blends with CdSe quantum dots since these blends are known to produce functional bulk heterojunction solar cells.

RESULTS AND DISCUSSION

For the purposes of IR sensitization, one would be interested in charge transfer from PbSe quantum dots to the polymer host. However, the purpose of this study is to determine if PbSe blends support photoinduced charge separation across the PbSe/conjugated polymer interface. Since charge transfer is supported in both directions for a type-II heterojunction, we first examine the change in the polymer photoluminescence intensity in polymer blend films incorporating PbSe quantum dots.[5,40]

Figure 1 shows the integrated polymer photoluminescence (PL) of both MDMO-PPV and P3HT as a function of PbSe quantum dot loading for blends of these two polymers with 3.5 nm diameter PbSe quantum dots. The quantum dots have been ligand-exchanged to replace the oleic acid leftover from the synthesis with butylamine, which has a shorter alkyl chain to facilitate charge transfer. At high PbSe loading, the PL from MDMO-PPV films (Figure 1A) quenches by nearly 80% relative to that of the pristine polymer film. Figure 1B, on the other hand, shows that blending PbSe quantum dots into P3HT films results in insignificant PL quenching; less than 20% of the PL is quenched even at high PbSe loadings. Though the MDMO-PPV blends show

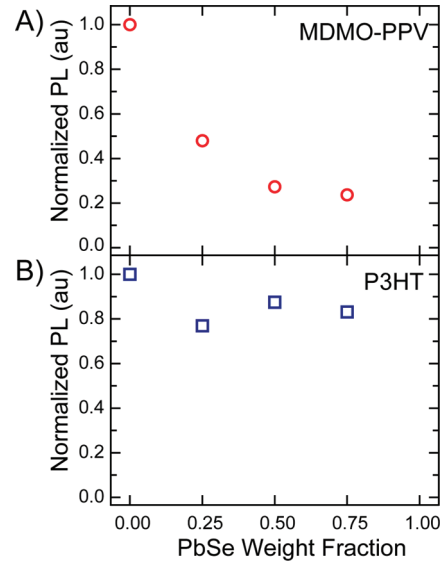

Figure 1. (A) MDMO-PPV and (B) P3HT integrated film PL as a function of quantum dot weight fraction.

fairly strong quenching, we attribute the small degree of quenching in the P3HT films to absorption or scattering of the 455 nm excitation light by the PbSe quantum dots, consistent with the UV−vis spectrum of the blend (Supporting Information Figure S1).

Figure 2 shows the time-resolved polymer PL decays for blend films of PbSe quantum dots with (A) MDMO-PPV and (B) P3HT, excited at 470 nm and measured using time-correlated single photon counting. The decays for the MDMO-PPV blends show a marked decrease in lifetime upon addition of PbSe quantum dots. This is consistent with the quenching exhibited in Figure 1A and demonstrates that the addition of PbSe quantum dots to MDMO-PPV films provides the polymer exciton with alternative relaxation pathways to PL. In contrast, the P3HT film PL lifetimes (Figure 2B)

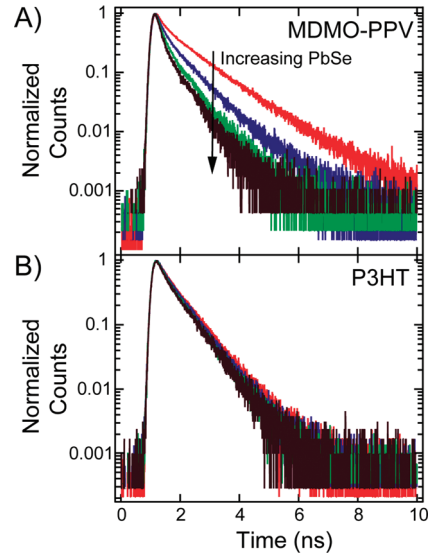

Figure 2. Polymer film PL decays for (A) PPV and (B) P3HT blends containing 0% (red), 25% (blue), 50% (green), and 75% (brown) PbSe QDs by weight.

do not exhibit a decrease upon addition of PbSe quantum dots. This is consistent with our hypothesis that the small amount of quenching observed in Figure 1B is due to absorption or scattering of the 455 nm excitation beam by the PbSe rather than by charge or energy transfer from the polymer to the PbSe host (PIA data for samples used in Figure 1 are in the Supporting Information, Figures S2−S4).

Though the MDMO-PPV films clearly show disruption of the normal radiative decay of the polymer excitons upon addition of PbSe quantum dots, PL quenching alone cannot differentiate between photoinduced charge transfer and other nonradiative decay pathways, such as energy transfer. Using only the PL results then, it is still difficult to determine if bulk heterojunction blends with PbSe are exhibiting poor photovoltaic performance due to lack of long-lived charge generation or some other mechanism, such as poor charge transport. Therefore, we employ quasi-steady-state photoinduced absorption (PIA) spectroscopy as a direct probe of charge transfer states.[40−46] Quasi-steady-state PIA monitors the change in the transmission spectrum of a film due to absorption by long-lived species (>10 μs) such as polarons and triplet excitons. When a conjugated polymer acts as an electron donor (or hole acceptor), a positive charge is created on the polymer backbone. This positive charge and the associated structural relaxation of the polymer backbone around it are collectively termed a positive polaron and exhibit characteristic subgap absorption spectra in conjugated polymers (Supporting Information, Scheme 1).[47] PIA probes these subgap absorptions, which provide a spectroscopic fingerprint of positive polarons and thus can confirm the occurrence of long-lived photoinduced charge transfer in bulk heterojunction blends. Photoinduced charge transfer can be followed by fast recombination,[48−50] but quasi-steady-state photoinduced absorption is useful in that it probes carriers with lifetimes long enough to be harvested in a photovoltaic cell.

Figure 3A shows the X-channel (in phase) PIA signal for three MDMO-PPV blends photoexcited at 455 nm with a modulation frequency of 200 Hz: the red circles are the data from the MDMO-PPV and PCBM blend; the blue squares are the MDMO-PPV and 3.8 nm CdSe blend; and the green diamonds are the MDMO-PPV with 3.5 nm PbSe blend. The spectra for blends of MDMO-PPV with PCBM and with CdSe quantum dots show a broad feature between 1.0 and 2.1 eV with a maximum at ~1.35 eV characteristic of the reported high-energy polaronic absorption spectra of alkoxy-PPVs[45] and similar to previously reported PIA spectra on CdSe blends with similar alkoxy-PPVs.[40,41] The onset of the low-energy polaron feature (which should peak farther into the IR) is also evident below 1 eV. In contrast to the spectra from CdSe and PCBM blends, no features are evident in the PbSe blend (green diamonds)

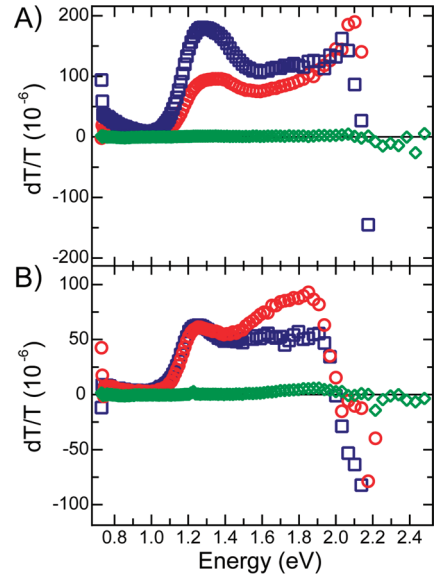

Figure 3. X-Channel PIA spectra for (A) PPV and (B) P3HT blends with PCBM (red circles), CdSe QDs (blue squares), and PbSe QDs (green diamonds).

above the noise of our experiment (2−3 ppm). This was observed for blends of MDMO-PPV with PbSe quantum dots ranging in size from 3.5 nm ($E_g \approx 1$ eV) to 4.8 nm ($E_g \approx 0.73$ eV).

Figure 3B shows the PIA spectra for the P3HT blends. Similar to the MDMO-PPV samples, we see strong polaronic features in the PIA spectra from both the PCBM (red circles) and 3.8 nm CdSe quantum dots (blue squares) blends with P3HT, but not for the blend with 3.5 nm PbSe quantum dots (green diamonds). The P3HT/PCBM and P3HT/CdSe spectra both have a broad absorption from 1.0 to 2.1 eV with a peak at ~1.25 eV. These spectra correspond well with previous literature reports on the polaronic absorption features in P3HT.[44] As with the MDMO-PPV blends, no characteristic P3HT polaron features are detected in the spectra from the PbSe blends above our noise limit. We observed no polaron features for any blends of P3HT with all PbSe quantum dots studied ranging in size from 3.5 nm ($E_g \approx 1$ eV) to 6 nm ($E_g \approx 0.69$ eV).

These PIA experiments put an upper limit on the amount of long-lived photoinduced charge that could be generated in both the P3HT and MDMO-PPV blends with the sizes of PbSe we studied. Considering the ~2−3 ppm noise in our experiment, we can make estimates for the maximum amount of charge generated in these blends relative to the blends of the polymers with PCBM and CdSe. Since the P3HT/PCBM and P3HT/CdSe blends consistently exhibit signals between 70 and 100 ppm, we conclude that the PCBM and CdSe blends are generating at least 30 times more long-lived charge than the PbSe blends. Similarly, the signal from the MDMO-PPV/PCBM and MDMO-PPV/CdSe blends peaks at 200 ppm, and we conclude that at least 60 times more long-lived charge is being generated in

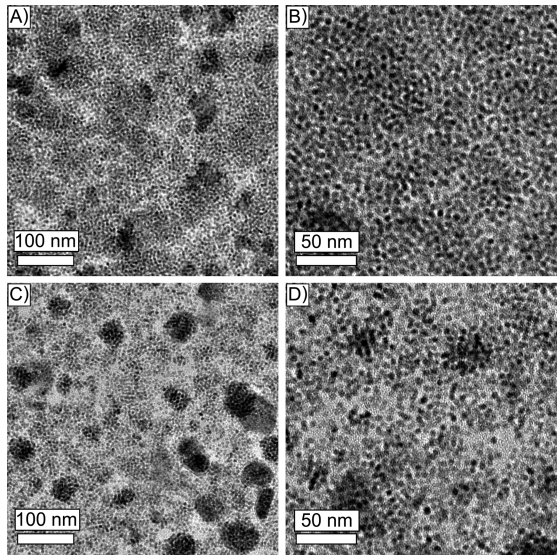

Figure 4. TEM images of (A,B) PPV/PbSe blend and of (C,D) P3HT/PbSe blend with 55% w/w PbSe. The P3HT films are ~30 nm thick, and the PPV films are ~20 nm thick.

MDMO-PPV blends with PCBM or CdSe compared with those using PbSe.

One explanation for the lack of a strong PIA signal in the polymer/PbSe blends could be that the PbSe quantum dots are phase separated on a length scale much larger than the exciton diffusion length, 4.5−6 nm in MDMO-PPV[51,52] and 5−8.5 nm in P3HT.[53−55] Although the polymer/PbSe blends are of good optical quality, showing little scattering that would be suggestive of large-scale phase separation, we also performed high-resolution transmission electron microscopy to examine the nanoscale morphology of the PbSe/polymer blends. Figure 4 shows TEM images of both PbSe/MDMO-PPV (Figure 4A,B) and PbSe/P3HT (Figure 4C,D) films spin-coated from the same solutions used to produce the films for the PIA data in Figure 3. Similar to previous reports of CdSe/polymer blends,[5,40,56] the PbSe nanoparticles show some aggregation, but a high loading is achieved, and there is extensive polymer/PbSe interfacial area to support photoinduced charge transfer. To explain the almost complete lack of PL quenching or long-lived polaronic PIA signals in the P3HT blends solely on the basis of morphology, most of the polymer volume would need to be contained in polymer domains that are free of any PbSe and are several tens of nanometers across. While some unmixed void areas are evident in Figures 4A−D, a far larger percentage of the film appears to contain PbSe quantum dots mixed on the 5−10 nm scale comparable to the reported exciton diffusion lengths for both polymers. Since these TEM micrographs appear similar to those reported for CdSe/polymer blends,[5,40,56] which do show significant PL quenching and PIA signals, we conclude that morphology alone cannot be the primary cause of the lack of spectroscopic signatures for charge transfer in these PbSe/polymer blends.

For the PbSe/P3HT blend, the absence of polymer PL quenching, the absence of any change in the polymer PL lifetime, and the lack of a detectable PIA signal all indicate that P3HT does not undergo either photoinduced charge transfer or energy transfer to PbSe quantum dots in the 3.5−6.0 nm size range. Since our quasi-steady-state PIA experiment probes only long-lived charges, it would not detect charge transfer followed by fast recombination. However, in such a case, we would expect to see quenching of the P3HT PL, accompanied by a decrease in the P3HT PL lifetime.

For the PbSe/MDMO-PPV blends, however, the lack of a detectable PIA signal in the presence of strong PL quenching and changes in the PL lifetime for the MDMO-PPV suggests two possible explanations. The PbSe/MDMO-PPV blend could be generating charge that is recombining on rapid time scales and is thus undetectable in our quasi-steady-state experiment. If true, the presence of a fast recombination pathway would also explain the poor device performance of PbSe/PPV blends. However, given the similarity in energy levels between the MDMO-PPV and P3HT polymers, we believe it unlikely that one polymer would support charge separation for the entire range of PbSe particle sizes studied while the other polymer does not exhibit charge transfer for PbSe quantum dots of any size.

A second, and in our view more likely, explanation for the observed PL quenching and lifetime changes in the MDMO-PPV/PbSe blends is energy transfer from the polymer to the PbSe. Förster resonance energy transfer (FRET) is a nonradiative, dipole−dipole interaction that depends on the overlap between the absorption spectrum of the acceptor with the fluorescence emission spectrum of the donor, close physical proximity between the two materials, and the donor's fluorescence quantum yield.[57] The first two criteria are met for both polymers, as the PbSe quantum dots absorb strongly in the visible range, across their emission spectra and, as discussed above and shown in Figure 4, the materials are blended in close proximity. Quenching by energy transfer for MDMO-PPV but not P3HT would also be consistent with the known differences in radiative lifetime for these two polymers. Given the known quantum yields and the measured PL lifetimes for P3HT and MDMO-PPV, it can be deduced that P3HT has a much longer (10−20×) radiative lifetime than MDMO-PPV (consistent with the formation of H-aggregates in P3HT films).[58] Since Förster transfer rates are inversely proportional to the radiative lifetime of the emitter,[57] we would expect much faster Förster transfer from MDMO-PPV to PbSe than from P3HT to PbSe.

CONCLUSIONS

We have studied charge transfer at the interface between PbSe quantum dots and the conjugated polymers MDMO-PPV and regioregular P3HT using photoluminescence and PIA spectroscopies. We have

contrasted the spectroscopic properties of the polymer/PbSe blends with polymer/CdSe and polymer/PCBM blends. While PbSe quantum dots quench the photoluminescence and decrease the photoluminescence lifetime of MDMO-PPV films, we observe no photoluminescence quenching or change in photoluminescence lifetime for the PbSe/P3HT blends. Photoinduced absorption spectra of both MDMO-PPV and P3HT blends with PbSe quantum dots show no evidence of long-lived photoinduced charge transfer between the PbSe quantum dots and either polymer. In contrast, blends of both polymers with either PCBM or CdSe quantum dots show PIA spectra indicative of long-lived polarons. We interpret these results as being consistent with energy transfer but not long-lived charge transfer in the MDMO-PPV/PbSe quantum dot blends and a near complete lack of either charge transfer or energy transfer in the P3HT/PbSe quantum dot blends. We thus infer that PbSe quantum dots do not form suitable junctions for photovoltaic applications with either MDMO-PPV or P3HT.

Although the wide range of reported LUMO positions for PbSe nanocrystals would suggest a large driving force exists for electron transfer from typical conjugated polymers to PbSe nanocrystals,[11,12,36,37] it is possible that interfacial chemistry effects (surface ligands, chemical changes in the PbSe surface, or polymer/PbSe interactions) either alter the relative band alignments in the solid state compared to solution measurements or present kinetic barriers to electron transfer from the polymer.

Our results suggest that the reason blends of PbSe quantum dots with widely studied polymers have so far performed poorly in bulk heterojunction devices compared to polymer/PCBM and polymer/CdSe blends is that there is little to no photoinduced generation of long-lived charge in PbSe/polymer systems.

Note Added in Proof. We recently learned that Tobias Hanrath and Rene A. Janssen have observed PL quenching in MDMO-PPV/PbSe blends consistent with our results[63] as well as polaron signals in PIA spectra of blends of P3HT and pyridine-treated PbSe.[64] This second observation could suggest that pyridine-capped and butylamine-capped quantum dots exhibit qualitatively different behavior; however, we have observed strong PIA signals with butylamine-capped CdSe in polymer blends (Supporting Information Figure S6). We thus believe the primary difference between the experiments is that their PIA spectra were conducted at cryogenic temperatures with larger signal to noise. The dT/T values from their polymer/PbSe blends[64] seem to be smaller than dT/T values from blends of polymers with PCBM,[65] with nanocrystalline ZnO,[66] and with nanocrystalline TiO_2[67] reported from the Janssen lab. We believe at this point that their results, showing smaller polymer polaron yields in PbSe blends relative to blends with other electron acceptors, are consistent with our own conclusions.

METHODS

Chemicals: Lead(II) oxide powder (PbO 99.999%), cadmium(II) oxide powder (CdO, 99.99+%), selenium powder (Se, ~100 mesh, 99.99%), trioctylphosphine (TOP), oleic acid (technical grade, 90%), octadecyl amine (ODA), *n*-trioctylphosphine oxide (TOPO, 90%), octadecene (ODE 90 and 95%), and butyl amine (>99.5%) were purchased from Sigma Aldrich. Pyridine and all of the solvents were purchased from EMD. MDMO-PPV was synthesized in house using a Gilch polymerization route *via* dehydrohalogenation of appropriate precursors as outlined in the literature.[59] P3HT (M_w = 50 000, rr = 90−93%) was purchased from Rieke Metals. PCBM (99.5%) was purchased from Nano-C.

Synthesis: We synthesized PbSe quantum dots using standard Schlenk line techniques and a protocol modified from Yu *et al.*[19] PbO (0.8920 g, 4.00 mmol), oleic acid (2.825 g, 10.00 mmol), and ODE (12.83 g, ~51 mmol) are stirred together in a three-neck flask and heated to 180 °C under continuous N_2 flow; 6.4 g of 10% w/w selenium solution in TOP is prepared in a nitrogen drybox. This selenium precursor solution is rapidly injected into the lead solution, dropping the temperature to about 150 °C, where it is set for the remainder of the growth process. The reaction is quenched by placing the reaction vessel in ice, rapidly dropping the temperature. The resulting solution is mixed with an approximately equal volume of acetone to precipitate the dots, which are then isolated by centrifugation (3000 rpm for 1 min). The precipitate is then dissolved in as little hexanes as possible, typically 3−4 mL. The hexanes solution is extracted three to five times in a separatory funnel using equal volumes of methanol. The final, purified product is isolated by precipitating with a large fraction of methanol, centrifuging, and drying under N_2 flow.

In a typical CdSe synthesis,[60,61] 0.077 g of CdO is heated to 220 °C with 0.68 g of oleic acid (90% Sigma Aldrich) in 2 g of (95%) ODE to form Cd-oleate, and when the solution turns clear, it is removed from heating and allowed to cool to room temperature. Subsequently, 1.5 g of ODA and 0.5 g of TOPO are added to the mixture and heated. When the solution reaches 280 °C, 3 g of Se-TBP solution (1.4 g Se, 3.84 g of *n*-tribuytlphosphine (TBP), 12.33 g of ODE previously prepared in a glovebox) is swiftly injected. The temperature is then lowered to 260 °C, and the quantum dots are grown at this temperature. Upon reaching the desired size, the solution is removed from heating. All reactions are performed under nitrogen on a Schlenk line. After cooling to <70 °C, the quantum dots are extracted with methanol and hexanes.

Quantum dots are characterized using UV/vis/NIR absorption spectroscopy with the first exciton peaks used to determine sizes of both PbSe[19] and CdSe quantum dots.[62]

Ligand Exchange: We exchange the oleic acid ligands with butyl amine, which presents a smaller barrier to charge transfer.[14] A typical PbSe ligand exchange is performed by dissolving a batch of washed quantum dots in butylamine to a concentration of ~50 mg/mL and sonicating for 30 min. They are then precipitated with ethanol or isopropyl alcohol, isolated with centrifugation (3000 rpm, 1 min), and partially dried with N_2(g). This process is performed three times total, and the dots are then dispersed in chloroform with the aid of sonication. If the solution appeared turbid, it was centrifuged and decanted to remove any undissolved material.

The ligands on the CdSe are similarly exchanged for pyridine. In a typical ligand exchange, a synthesis batch is dispersed in hexanes (~100 mg/mL) and precipitated with methanol three times. The resulting precipitate is dried and then sonicated in py-

ridine for ~1 h. The solution is precipitated with hexanes, and the process is performed a total of three times.[5,40]

Film Processing: Concentrations of all polymer, PCBM, and quantum dot solutions were determined by evaporating known volumes to dryness and weighing the remaining material. Polymer/PCBM and polymer/QD films were spin-coated from distilled chloroform solutions in a nitrogen drybox. The films were loaded into a sealed sample chamber inside the drybox, and the chamber was immediately vacuum pumped to below 10 mTorr before beginning measurements. The films are kept under dynamic vacuum, at pressures lower than 10 mTorr, throughout the PIA and PL experiments.

PL and PIA Spectroscopy: PL and PIA spectra were measured simultaneously using standard lock-in techniques.[40] A 455 nm LED was electronically modulated by an Agilent 33120A Arbitrary Waveform Generator and a home-built driver circuit and was used to optically pump the sample while the change in transmitted light induced by the pump was probed with a monochromated tungsten lamp. A Si/InGaAs photodetector with sensitivity from the visible to the near-IR coupled with an SR830 lock-in amplifier was used to detect these changes, which are reported as d*T*/*T* values. The phase of the lock-in was set such that polymer PL or scattered LED pump light appeared entirely as a positive signal in the X-channel. Thus, a fast absorption induced by the pump appears as a negative d*T*/*T* signal in the X-channel. Corrections were made to subtract any film PL or scattered pump light from the PIA spectra.

PL Lifetimes: Fluorescence decays of the blend thin films were obtained using the time-correlated single photon counting (TCSPC) technique on a PicoQuant FluoTime 100 spectrometer equipped with a PicoHarp 300 TCSPC module. The instrument utilizes a fast Hamamatsu (model PMA 182-N) photomultiplier tube as the detector and a 470 nm pulsed diode laser (LDH-P-C-470, PicoQuant) as the excitation source. The decay curves were analyzed using the FluoFit software package provided by PicoQuant. Reduced χ^2 values, weighted residuals, and autocorrelation of the residuals were used as the goodness-of-fit criteria. All decay curves measured were adequately described by a double-exponential model. Single-exponential lifetime distribution and stretched exponential models each gave poorer fits. All measurements were done at room temperature under N_2 flow.

Acknowledgment. This paper is based on work supported by the National Science Foundation (DMR-0120967 and DMR-0449422) and work supported by the Department Of Energy. D.G. also thanks the Camille Dreyfus Teacher-Scholar Awards Program for support. D.G. is a Cottrell Scholar of the Research Corporation and an Alfred P. Sloan Foundation Research Fellow. N.A. is a Washington Research Foundation Fellow, and N.A. and N.H. are both Mary Gates Scholars.

Note added after ASAP publication: An older version of Supporting Information was published with this article May 18, 2009. The correct version was published May 20, 2009.

Supporting Information Available: UV−vis absorption spectra of MDMO-PPV and P3HT films used for Figure 1. X-Channel PIA of the "0.75 PbSe Loading" data point in Figure 1A, exhibiting no polaronic signature. X-Channel PIA data for all PPV samples in Figure 1A and the P3HT samples in Figure 1B scaled for clarity. Absorption spectra of PbSe QDs used in this work. One electron energy level scheme for PIA. This material is available free of charge *via* the Internet at http://pubs.acs.org.

REFERENCES AND NOTES

1. Shaheen, S. E.; Ginley, D. S.; Jabbour, G. E. Organic-Based Photovoltaics. Toward Low-Cost Power Generation. *MRS Bull.* **2005**, *30*, 10–19.
2. Munro, A. M.; Bardecker, J. A.; Liu, M. S.; Cheng, Y. J.; Niu, Y. H.; Plante, I. J. L.; Jen, A. K. Y.; Ginger, D. S. Colloidal CdSe Quantum Dot Electroluminescence: Ligands and Light-Emitting Diodes. *Microchim. Acta* **2008**, *160*, 345–350.
3. Niu, Y. H.; Munro, A. M.; Cheng, Y. J.; Tian, Y. Q.; Liu, M. S.; Zhao, J. L.; Bardecker, J. A.; Plante, I. J. L.; Ginger, D. S.; Jen, A. K. Y. Improved Performance Light-Emitting Diodes Quantum Dot Layer. *Adv. Mater.* **2007**, *19*, 3371.
4. Zhao, J. L.; Bardecker, J. A.; Munro, A. M.; Liu, M. S.; Niu, Y. H.; Ding, I. K.; Luo, J. D.; Chen, B. Q.; Jen, A. K. Y.; Ginger, D. S. Efficient CdSe/CdS Quantum Dot Light-Emitting Diodes Using a Thermally Polymerized Hole Transport Layer. *Nano Lett.* **2006**, *6*, 463–467.
5. Greenham, N. C.; Peng, X. G.; Alivisatos, A. P. Charge Separation and Transport in Conjugated-Polymer/Semiconductor-Nanocrystal Composites Studied by Photoluminescence Quenching and Photoconductivity. *Phys. Rev. B* **1996**, *54*, 17628–17637.
6. Huynh, W. U.; Dittmer, J. J.; Alivisatos, A. P. Hybrid Nanorod-Polymer Solar Cells. *Science* **2002**, *295*, 2425–2427.
7. Zhou, Y.; Li, Y. C.; Zhong, H. Z.; Hou, J. H.; Ding, Y. Q.; Yang, C. H.; Li, Y. F. Hybrid Nanocrystal/Polymer Solar Cells Based on Tetrapod-Shaped $CdSe_xTe_{1-x}$ Nanocrystals. *Nanotechnology* **2006**, *17*, 4041–4047.
8. Gur, I.; Fromer, N. A.; Chen, C. P.; Kanaras, A. G.; Alivisatos, A. P. Hybrid Solar Cells with Prescribed Nanoscale Morphologies Based on Hyperbranched Semiconductor Nanocrystals. *Nano Lett.* **2007**, *7*, 409–414.
9. Milliron, D. J.; Gur, I.; Alivisatos, A. P. Hybrid Organic−Nanocrystal Solar Cells. *MRS Bull.* **2005**, *30*, 41–44.
10. Biebersdorf, A.; Dietmuller, R.; Susha, A. S.; Rogach, A. L.; Poznyak, S. K.; Talapin, D. V.; Weller, H.; Klar, T. A.; Feldmann, J. Semiconductor Nanocrystals Photosensitize C-60 Crystals. *Nano Lett.* **2006**, *6*, 1559–1563.
11. Cui, D. H.; Xu, J.; Zhu, T.; Paradee, G.; Ashok, S.; Gerhold, M. Harvest of Near Infrared Light in PbSe Nanocrystal-Polymer Hybrid Photovoltaic Cells. *Appl. Phys. Lett.* **2006**, *88*, 3.
12. Jiang, X. M.; Schaller, R. D.; Lee, S. B.; Pietryga, J. M.; Klimov, V. I.; Zakhidov, A. A. PbSe Nanocrystal/Conducting Polymer Solar Cells with an Infrared Response to 2 Micron. *J. Mater. Res.* **2007**, *22*, 2204–2210.
13. Günes, S.; Fritz, K. P.; Neugebauer, H.; Sariciftci, N. S.; Kumar, S.; Scholes, G. D. Hybrid Solar Cells Using PbS Nanoparticles. *Sol. Energy Mater. Sol. Cells* **2007**, *91*, 420–423.
14. McDonald, S. A.; Konstantatos, G.; Zhang, S. G.; Cyr, P. W.; Klem, E. J. D.; Levina, L.; Sargent, E. H. Solution-Processed PbS Quantum Dot Infrared Photodetectors and Photovoltaics. *Nat. Mater.* **2005**, *4*, 138–142.
15. Zhang, S.; Cyr, P. W.; McDonald, S. A.; Konstantatos, G.; Sargent, E. H. Enhanced Infrared Photovoltaic Efficiency in PbS Nanocrystal/Semiconducting Polymer Composites: 600-fold Increase in Maximum Power Output *via* Control of the Ligand Barrier. *Appl. Phys. Lett.* **2005**, *87*, 233101.
16. Talapin, D. V.; Murray, C. B. PbSe Nanocrystal Solids for n- and p-Channel Thin Film Field-Effect Transistors. *Science* **2005**, *310*, 86–89.
17. Cademartiri, L.; Bertolotti, J.; Sapienza, R.; Wiersma, D. S.; von Freymann, G.; Ozin, G. A. Multigram Scale, Solventless, and Diffusion-Controlled Route to Highly Monodisperse PbS Nanocrystals. *J. Phys. Chem. B* **2006**, *110*, 671–673.
18. Murphy, J. E.; Beard, M. C.; Norman, A. G.; Ahrenkiel, S. P.; Johnson, J. C.; Yu, P. R.; Micic, O. I.; Ellingson, R. J.; Nozik, A. J. PbTe Colloidal Nanocrystals: Synthesis, Characterization, and Multiple Exciton Generation. *J. Am. Chem. Soc.* **2006**, *128*, 3241–3247.
19. Yu, W. W.; Falkner, J. C.; Shih, B. S.; Colvin, V. L. Preparation and Characterization of Monodisperse PbSe Semiconductor Nanocrystals in a Noncoordinating Solvent. *Chem. Mater.* **2004**, *16*, 3318–3322.
20. Schaller, R. D.; Sykora, M.; Pietryga, J. M.; Klimov, V. I. Seven Excitons at a Cost of One: Redefining the Limits for Conversion Efficiency of Photons into Charge Carriers. *Nano Lett.* **2006**, *6*, 424–429.
21. Shabaev, A.; Efros, A. L.; Nozik, A. J. Multiexciton Generation by a Single Photon in Nanocrystals. *Nano Lett.* **2006**, *6*, 2856–2863.

22. Nair, G.; Geyer, S. M.; Chang, L. Y.; Bawendi, M. G. Carrier Multiplication Yields in PbS and PbSe Nanocrystals Measured by Transient Photoluminescence. *Phys. Rev. B* **2008**, 78.
23. Nair, G.; Bawendi, M. G. Carrier multiplication yields of CdSe and CdTe nanocrystals by transient photoluminescence spectroscopy. *Phys. Rev. B* **2007**, 76.
24. Ben-Lulu, M.; Mocatta, D.; Bonn, M.; Banin, U.; Ruhman, S. On the Absence of Detectable Carrier Multiplication in a Transient Absorption Study of InAs/CdSe/ZnSe Core/Shell1/Shell2 Quantum Dots. *Nano Lett.* **2008**, *8*, 1207–1211.
25. Trinh, M. T.; Houtepen, A. J.; Schins, J. M.; Hanrath, T.; Piris, J.; Knulst, W.; Goossens, A. P. L. M.; Siebbeles, L. D. A. In Spite of Recent Doubts Carrier Multiplication Does Occur in PbSe Nanocrystals. *Nano Lett.* **2008**, *8*, 1713–1718.
26. McGuire, J. A.; Joo, J.; Pietryga, J. M.; Schaller, R. D.; Klimov, V. I. New Aspects of Carrier Multiplication in Semiconductor Nanocrystals. *Acc. Chem. Res.* **2008**, *41*, 1810–1819.
27. Hwang, I. W.; Cho, S.; Kim, J. Y.; Lee, K.; Coates, N. E.; Moses, D.; Heeger, A. J. Carrier Generation and Transport in Bulk Heterojunction Films Processed with 1,8-Octanedithiol as a Processing Additive. *J. Appl. Phys.* **2008**, *104*, 033706.
28. Noone, K. M.; Ginger, D. S. Doping for Speed: Colloidal Nanoparticles for Thin-Film Optoelectronics. *ACS Nano* **2009**, *3*, 261–265.
29. Clifford, J. P.; Johnston, K. W.; Levina, L.; Sargent, E. H. Schottky Barriers to Colloidal Quantum Dot Films. *Appl. Phys. Lett.* **2007**, *91*, 253117-3.
30. Johnston, K. W.; Pattantyus-Abraham, A. G.; Clifford, J. P.; Myrskog, S. H.; MacNeil, D. D.; Levina, L.; Sargent, E. H. Schottky-Quantum Dot Photovoltaics for Efficient Infrared Power Conversion. *Appl. Phys. Lett.* **2008**, *92*, 151115-3.
31. Koleilat, G. I.; Levina, L.; Shukla, H.; Myrskog, S. H.; Hinds, S.; Pattantyus-Abraham, A. G.; Sargent, E. H. Efficient, Stable Infrared Photovoltaics Based on Solution-Cast Colloidal Quantum Dots. *ACS Nano* **2008**, *2*, 833–840.
32. Kim, S. J.; Kim, W. J.; Sahoo, Y.; Cartwright, A. N.; Prasad, P. N. Multiple Exciton Generation and Electrical Extraction from a PbSe Quantum Dot Photoconductor. *Appl. Phys. Lett.* **2008**, *92*, 3.
33. Luther, J. M.; Law, M.; Beard, M. C.; Song, Q.; Reese, M. O.; Ellingson, R. J.; Nozik, A. J. Schottky Solar Cells Based on Colloidal Nanocrystal Films. *Nano Lett.* **2008**, *8*, 3488–3492.
34. Kim, S. J.; Kim, W. J.; Cartwright, A. N.; Prasad, P. N. Carrier Multiplication in a PbSe Nanocrystal and P3HT/PCBM Tandem Cell. *Appl. Phys. Lett.* **2008**, *92*, 3.
35. Forrest, S. R. The Limits to Organic Photovoltaic Cell Efficiency. *MRS Bull.* **2005**, *30*, 28–32.
36. Solomeshch, O.; Kigel, A.; Saschiuk, A.; Medvedev, V.; Aharoni, A.; Razin, A.; Eichen, Y.; Banin, U.; Lifshitz, E.; Tessler, N. Optoelectronic Properties of Polymer-Nanocrystal Composites Active at Near-Infrared Wavelengths. *J. Appl. Phys.* **2005**, *98*, 074310.
37. Hyun, B.-R.; Zhong, Y.-W.; Bartnik, A. C.; Sun, L.; Abruña, H. D.; Wise, F. W.; Goodreau, J. D.; Matthews, J. R.; Leslie, T. M.; Borrelli, N. F. Electron Injection from Colloidal PbS Quantum Dots into Titanium Dioxide Nanoparticles. *ACS Nano* **2008**, *2*, 2206–2212.
38. Aldakov, D.; Chandezon, F.; De Bettignies, R.; Firon, M.; Reiss, P.; Pron, A. Hybrid Organic-Inorganic Nanomaterials: Ligand Effects. *Eur. Phys. J.: Appl. Phys.* **2006**, *36*, 261–265.
39. Soreni-Hararl, M.; Yaacobi-Gross, N.; Steiner, D.; Aharoni, A.; Banin, U.; Millo, O.; Tessler, N. Tuning Energetic Levels in Nanocrystal Quantum Dots Through Surface Manipulations. *Nano Lett.* **2008**, *8*, 678–684.
40. Ginger, D. S.; Greenham, N. C. Photoinduced Electron Transfer from Conjugated Polymers to CdSe Nanocrystals. *Phys. Rev. B* **1999**, *59*, 10622–10629.
41. Ginger, D. S.; Greenham, N. C. Charge Separation in Conjugated-Polymer/Nanocrystal Blends. *Synth. Met.* **1999**, *101*, 425–428.
42. Comoretto, D.; Moggio, I.; Cuniberti, C.; Musso, G. F.; Dellepiane, G.; Borghesi, A.; Kajzar, F.; Lorin, A. Long-Lived Photoexcited States in Polydiacetylenes: The Photoinduced-Absorption Spectra of PDA-4BCMU. *Phys. Rev. B* **1998**, *57*, 7071–7078.
43. Silva, C.; Russell, D. M.; Dhoot, A. S.; Herz, L. M.; Daniel, C.; Greenham, N. C.; Arias, A. C.; Setayesh, S.; Mullen, K.; Friend, R. H. Exciton and Polaron Dynamics in a Step-Ladder Polymeric Semiconductor: The Influence of Interchain Order. *J. Phys.: Condens. Matter* **2002**, *14*, 9803–9824.
44. Österbacka, R.; An, C. P.; Jiang, X. M.; Vardeny, Z. V. Two-Dimensional Electronic Excitations in Self-Assembled Conjugated Polymer Nanocrystals. *Science* **2000**, *287*, 839–842.
45. Wei, X.; Vardeny, Z. V.; Sariciftci, N. S.; Heeger, A. J. Absorption-Detected Magnetic-Resonance Studies of Photoexcitations in Conjugated-Polymer/C60 Composites. *Phys. Rev. B* **1996**, *53*, 2187–2190.
46. Ginger, D. S.; Dhoot, A. S.; Finlayson, C. E.; Greenham, N. C. Long-Lived Quantum-Confined Infrared Transitions in CdSe Nanocrystals. *Appl. Phys. Lett.* **2000**, *77*, 2816–2818.
47. Bredas, J. L.; Street, G. B. Polarons, Bipolarons, and Solitons in Conducting Polymers. *Acc. Chem. Res.* **1985**, *18*, 309–315.
48. Hwang, I. W.; Moses, D.; Heeger, A. J. Photoinduced Carrier Generation in P3HT/PCBM Bulk Heterojunction Materials. *J. Phys. Chem. C* **2008**, *112*, 4350–4354.
49. Ohkita, H.; Cook, S.; Astuti, Y.; Duffy, W.; Tierney, S.; Zhang, W.; Heeney, M.; McCulloch, I.; Nelson, J.; Bradley, D. D. C.; Durrant, J. R. Charge Carrier Formation in Polythiophene/Fullerene Blend Films Studied by Transient Absorption Spectroscopy. *J. Am. Chem. Soc.* **2008**, *130*, 3030–3042.
50. Russell, D. M.; Arias, A. C.; Friend, R. H.; Silva, C.; Ego, C.; Grimsdale, A. C.; Mullen, K. Efficient Light Harvesting in a Photovoltaic Diode Composed of a Semiconductor Conjugated Copolymer Blend. *Appl. Phys. Lett.* **2002**, *80*, 2204–2206.
51. Scully, S. R.; McGehee, M. D. Effects of Optical Interference and Energy Transfer on Exciton Diffusion Length Measurements in Organic Semiconductors. *J. Appl. Phys.* **2006**, *100*, 034907.
52. Mikhnenko, O. V.; Cordella, F.; Sieval, A. B.; Hummelen, J. C.; Blom, P. W. M.; Loi, M. A. Temperature Dependence of Exciton Diffusion in Conjugated Polymers. *J. Phys. Chem. B* **2008**, *112*, 11601–11604.
53. Goh, C.; Scully, S. R.; McGehee, M. D. Effects of Molecular Interface Modification in Hybrid Organic-Inorganic Photovoltaic Cells. *J. Appl. Phys.* **2007**, *101*, 114503.
54. Kroeze, J. E.; Savenije, T. J.; Vermeulen, M. J. W.; Warman, J. M. Contactless Determination of the Photoconductivity Action Spectrum, Exciton Diffusion Length, and Charge Separation Efficiency in Polythiophene-Sensitized TiO_2 Bilayers. *J. Phys. Chem. B* **2003**, *107*, 7696–7705.
55. Shaw, P. E.; Ruseckas, A.; Samuel, I. D. W. Exciton Diffusion Measurements in Poly(3-hexylthiophene). *Adv. Mater.* **2008**, *20*, 3516–3520.
56. Huynh, W. U.; Dittmer, J. J.; Libby, W. C.; Whiting, G. L.; Alivisatos, A. P. Controlling the Morphology of Nanocrystal-Polymer Composites for Solar Cells. *Adv. Funct. Mater.* **2003**, *13*, 73–79.
57. Pope, M.; Swenberg, C. E. *Electronic Process in Organic Crystals and Polymers*; Oxford University Press: New York, 1999; pp 96−101.
58. Clark, J.; Silva, C.; Friend, R. H.; Spano, F. C. Role of Intermolecular Coupling in the Photophysics of Disordered Organic Semiconductors: Aggregate Emission in Regioregular Polythiophene. *Phys. Rev. Lett.* **2007**, *98*, 206406.
59. Becker, H.; Spreitzer, H.; Ibrom, K.; Kreuder, W. New Insights into the Microstructure of GILCH-Polymerized PPVs. *Macromolecules* **1999**, *32*, 4925–4932.
60. Qu, L.; Peng, Z. A.; Peng, X. Alternative Routes toward High Quality CdSe Nanocrystals. *Nano Lett.* **2001**, *1*, 333–337.

61. Munro, A. M.; Jen-La Plante, I.; Ng, M. S.; Ginger, D. S. Quantitative Study of the Effects of Surface Ligand Concentration on CdSe Nanocrystal Photoluminescence. *J. Phys. Chem. C* **2007**, *111*, 6220–6227.
62. Yu, W. W.; Qu, L. H.; Guo, W. Z.; Peng, X. G. Experimental Determination of the Extinction Coefficient of CdTe, CdSe, and CdS Nanocrystals. *Chem. Mater.* **2003**, *15*, 2854–2860.
63. Hanrath, T.; Veldman, D.; Choi, J. J.; Christova, C. G.; Wienk, M. M.; Janssen, R. A. J. PbSe Nanocrystal Network Formation during Pyridine Ligand Displacement. *ACS Appl. Mater. Interfaces* **2009**, *1*, 244–250.
64. T. Hanrath, unpublished, Cornell University, private communication.
65. Offermans, T.; Meskers, S. C. J.; Janssen, R. A. J. Photoinduced Absorption Spectroscopy on MDMO-PPV: PCBM Solar Cells under Operation. *Org. Electron* **2007**, *8*, 325–335.
66. Beek, W. J. E.; Wienk, M. M.; Kemerink, M.; Yang, X.; Janssen, R. A. J. Hybrid Zinc Oxide Conjugated Polymer Bulk Heterojunction Solar Cells. *J. Phys. Chem. B* **2005**, *109*, 9505–9516.
67. van Hal, P. A.; Christiaans, M. P. T.; Wienk, M. M.; Kroon, J. M.; Janssen, R. A. J. Photoinduced Electron Transfer from Conjugated Polymers to TiO_2. *J. Phys. Chem. B* **1999**, *103*, 4352–4359.